

NRC 22643

INFRARED AND FAR-INFRARED TRANSITION FREQUENCIES FOR THE CH<sub>2</sub> RADICAL<sup>1</sup>

TREVOR J. SEARS, A. R. W. MCKELLAR, AND P. R. BUNKER  
Herzberg Institute of Astrophysics, National Research Council of Canada

K. M. EVENSON  
National Bureau of Standards

AND

J. M. BROWN  
Department of Chemistry, Southampton University  
Received 1983 May 13; accepted 1983 June 14

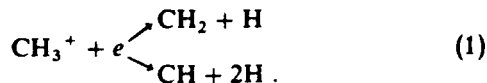
ABSTRACT

Frequencies, wavelengths, and line strengths for transitions of the CH<sub>2</sub> molecule at far-infrared and mid-infrared (9-12 μm) wavelengths have been calculated from recently reported laser magnetic resonance spectra.

Subject headings: infrared: spectra — interstellar: molecules — laboratory spectra — line identifications — transition probabilities

Methylene, CH<sub>2</sub>, is a very likely constituent of interstellar gas clouds where many other such reactive species have been detected. It has not been detected in astronomical sources, principally because, until recently, precise spectroscopic measurements for the triplet ground electronic state did not exist. Also, most of the transitions likely to occur in astronomical sources are in the relatively unexplored mid- and far-infrared wavelength regions. This paper presents a list of frequencies and intensities for transitions of CH<sub>2</sub> in the mid- and far-infrared regions which should aid in its detection and thus provide valuable information on the local physical and chemical environment.

In the case of dark molecular clouds, recent astrochemical calculations (Prasad and Huntress 1980; Inglesias 1977) have predicted CH<sub>2</sub> abundances of the same order of magnitude as those of CH. These models predict that the primary formation mechanism for both CH<sub>2</sub> and CH is via dissociative recombination of CH<sub>3</sub><sup>+</sup> and an electron



<sup>1</sup> Work supported in part by NASA contract W15047.

Measurements of CH<sub>2</sub> abundances will therefore lead to an estimate of the branching ratio for reaction (1) since the primary loss mechanism for both CH<sub>2</sub> and CH is thought to be the reaction with oxygen atoms.

The paucity of laboratory data on CH<sub>2</sub> in its <sup>3</sup>B<sub>1</sub> ground electronic state has recently been changed by the observation of vibrational spectra in the infrared (Sears, Bunker, and McKellar 1981, 1982) and rotational spectra in the far-infrared (Sears *et al.* 1982) regions by laser magnetic resonance (LMR) spectroscopy. Subsequently, one lower frequency rotational transition has been detected around 70 GHz by conventional microwave techniques (Lovas, Suenram, and Evenson 1983). In the LMR experiments the molecular transition frequency is tuned into coincidence with a fixed frequency laser by means of a variable magnetic field. Although the zero field frequencies are not measured directly in LMR, the data are of high quality and the theory of the Zeeman effect is sufficiently well understood (Sears *et al.* 1982) that the extrapolation to zero field can be performed reliably.

Table 1 lists the lowest few rotational energy levels of CH<sub>2</sub> in its ground electronic state. The asymmetric top energy levels, denoted by N<sub>K<sub>a</sub>K<sub>c</sub></sub>, are split into levels with J = N - 1, N, and N + 1 by fine structure interactions. Half the levels (those

TABLE 1  
LOW-LYING ROTATIONAL LEVELS OF CH<sub>2</sub> (IN GHz)

N <sub>K<sub>a</sub>K<sub>c</sub></sub>	J = N - 1			J = N			J = N + 1		
	F = N - 2	F = N - 1	F = N	F = N - 1	F = N	F = N + 1	F = N	F = N + 1	F = N + 2
0 <sub>00</sub>	...	...	...	...	...	...	-0.046	-0.066	-0.107
1 <sub>01</sub>	...	453.393	...	...	476.590	...	...	466.922	...
1 <sub>11</sub>	...	...	2354.687	2344.651	2344.631	2344.590	2348.555	2348.538	2348.514
1 <sub>10</sub>	...	2392.938	...	...	2379.266	...	...	2384.582	...
2 <sub>02</sub>	1397.897	1397.927	1397.986	1413.163	1413.169	1413.179	1402.743	1402.712	1402.670
2 <sub>12</sub>	...	3247.474	...	...	3256.093	...	...	3249.965	...
2 <sub>11</sub>	3356.025	3356.045	3356.086	3362.257	3362.257	3362.258	3357.651	3357.625	3357.590
3 <sub>03</sub>	...	2802.552	...	...	2816.133	...	...	2805.139	...
3 <sub>13</sub>	4601.350	4601.379	4601.423	4612.552	4612.555	4612.558	4603.504	4603.474	4603.436
3 <sub>12</sub>	...	4816.668	...	...	4825.628	...	...	4818.069	...
4 <sub>04</sub>	4670.358	4670.394	4670.442	4683.229	4683.233	4683.238	4671.884	4671.850	4671.808

TABLE 2  
CALCULATED ROTATIONAL TRANSITION FREQUENCIES FOR CH<sub>2</sub> (<sup>3</sup>B<sub>1</sub>)

$N_{k_a k_c}$	$J$	$F^a$	Frequency (GHz)	Vacuum Wavelength ( $\mu\text{m}$ )	Line Strength	$N_{k_a k_c}$	$J$	$F^a$	Frequency (GHz)	Vacuum Wavelength ( $\mu\text{m}$ )	Line Strength	
111-000	1-1	2-1	2344.657	127.862	0.82	220-111 <sup>b</sup>	2-1	3-2	3203.436	93.585	3.32	
	1-1	1-0	2344.677	127.861	0.66		2-1	2-1	3203.452	93.584	1.78	
	1-1	1-1	2344.697	127.860	0.51		2-1	1-0	3203.453	93.584	0.79	
	1-1	2-2	2344.697	127.860	2.53		3-3	4-4	3209.888	93.397	0.52	
	1-1	0-1	2344.717	127.859	0.67		2-2	3-3	5927.012	50.581	0.96	
	1-1	1-2	2344.738	127.858	0.84		2-2	2-2	5927.016	50.581	0.53	
	2-1	1-0	2348.601	127.647	1.12		2-1	2-1	5930.924	50.547	1.71	
	2-1	2-1	2348.605	127.647	2.52		2-1	1-0	5930.924	50.547	0.76	
	2-1	1-1	2348.621	127.646	0.83		2-1	3-2	5930.935	50.547	3.20	
	2-1	3-2	2348.621	127.646	4.66		2-1	1-1	5930.944	50.547	0.58	
	2-1	2-2	2348.645	127.645	0.81		2-1	2-2	5930.965	50.547	0.58	
	0-1	1-1	2354.753	127.314	0.66		1-0	2-1	5936.587	50.499	1.69	
	0-1	1-2	2354.793	127.312	1.10		1-0	1-1	5936.606	50.499	1.01	
	110-101	1-1	...	1902.677	157.564		0.73	3-2	2-1	5936.939	50.496	2.54
		2-1	...	1907.992	157.125		1.23	3-2	3-2	5936.947	50.496	3.77
		1-2	...	1912.343	156.767		1.24	3-2	4-3	5936.959	50.496	5.44
0-1		...	1916.348	156.439	1.00	1-1	2-2	5946.683	50.413	0.92		
2-2		...	1917.659	156.332	3.77	2-2	...	5890.416	50.895	0.76		
1-0		...	1925.873	155.666	1.03	2-1	...	5895.732	50.849	2.27		
212-101	1-1	...	2770.884	108.194	0.77	1-0	...	5897.774	50.831	1.00		
	2-1	...	2779.503	107.858	2.27	3-2	...	5900.339	50.809	4.19		
	3-2	...	2783.043	107.721	4.20	1-1	...	5911.447	50.714	0.73		
	2-2	...	2789.170	107.484	0.73	2-3	...	439.960	681.409	1.68		
1-0	...	2794.080	107.296	0.97	3-4	...	444.826	673.955	2.44			
111-202	1-2	2-3	931.412	321.869	0.99	1-2	...	444.922	673.810	1.14		
	1-2	1-2	931.462	321.852	0.53	2-3	...	2000.535	149.856	0.58		
	2-3	1-2	945.812	316.968	0.82	4-3	...	2001.936	149.751	0.57		
	2-3	2-3	945.827	316.963	1.21	3-3	...	2009.495	149.188	6.03		
	2-3	3-4	945.844	316.958	1.76	4-4	...	2012.929	148.933	8.66		
211-202	0-1	1-2	956.700	313.361	0.55	2-2	...	2014.116	148.846	4.55		
	1-2	1-2	1942.875	154.303	0.58	3-4	...	2020.488	148.376	0.57		
	1-2	2-3	1942.906	154.301	1.09	3-2	...	2023.076	148.186	0.58		
	3-2	4-3	1944.411	154.182	1.00	4-3	...	3601.793	83.234	4.62		
	3-2	3-2	1944.455	154.178	0.69	5-4	...	3602.298	83.223	6.02		
	2-2	2-3	1949.078	153.812	0.54	3-2	...	3603.534	83.194	3.51		
	2-2	3-3	1949.079	153.812	4.37	3-2	...	6443.446	46.527	3.07		
	2-2	2-2	1949.088	153.812	2.44	4-3	...	6449.224	46.485	4.41		
	2-2	3-2	1949.088	153.812	0.54	2-1	...	6452.472	46.462	2.05		
	2-2	1-2	1949.088	153.812	0.52	2-2	3-3	4913.268	61.017	1.37		
	2-2	2-1	1949.094	153.811	0.52	2-2	2-2	4913.298	61.017	0.77		
	2-2	1-1	1949.094	153.811	1.58	3-3	2-2	4927.843	60.836	1.28		
	3-3	4-3	1954.879	153.356	0.51	3-3	3-3	4927.860	60.836	1.69		
	3-3	3-2	1954.882	153.356	0.50	3-3	4-4	4927.883	60.836	2.43		
	3-3	2-2	1954.908	153.354	4.00	1-1	2-2	4935.188	60.746	0.93		
	3-3	3-3	1954.913	153.353	5.29	404-313 <sup>c</sup>	5-4	6-5	68.371	4384.740	4.00	
	3-3	4-4	1954.921	153.353	7.59		5-4	5-4	68.375	4384.486	3.25	
	3-3	2-3	1954.940	153.351	0.50		5-4	4-3	68.380	4384.194	2.64	
	3-3	3-4	1954.955	153.350	0.51		3-2	2-1	69.008	4344.337	1.19	
	1-1	1-2	1958.059	153.107	0.94		3-2	3-2	69.015	4343.881	1.76	
1-1	0-1	1958.098	153.104	0.75	3-2	4-3	69.020	4343.577	2.54			
1-1	2-2	1958.099	153.104	2.81	4-3	3-2	70.677	4241.724	1.85			
1-1	1-1	1958.118	153.102	0.56	4-3	4-3	70.679	4241.634	2.43			
1-1	1-0	1958.148	153.100	0.75	4-3	5-4	70.680	4241.535	3.17			
1-1	2-1	1958.159	153.099	0.95	220-313 <sup>b</sup>	3-4	4-5	3682.037	81.420	0.53		
2-3	2-3	1959.545	152.991	0.69		3-3	4-4	5084.229	58.965	2.99		
2-3	3-4	1959.588	152.987	0.99		3-3	3-3	5084.236	58.965	2.05		
2-1	3-2	1964.271	152.623	1.08		3-3	2-2	5084.243	58.965	1.54		
2-1	2-1	1964.330	152.618	0.58		4-4	3-3	5092.926	58.864	2.57		
313-202 <sup>b</sup>	2-2	3-3	3188.244	94.031	0.56	4-4	4-4	5092.935	58.864	3.18		
	3-2	4-3	3199.379	93.703	4.56	4-4	5-5	5092.948	58.864	4.17		
	3-2	3-2	3199.385	93.703	3.16	2-2	3-3	5095.736	58.832	2.35		
	3-2	2-1	3199.389	93.703	2.13	2-2	2-2	5095.760	58.832	1.32		
	4-3	3-2	3200.761	93.663	3.65	2-2	1-1	5095.774	58.832	0.84		
	4-3	4-3	3200.763	93.663	4.79	413-404	3-4	4-5	2079.944	144.135	0.57	
	4-3	5-4	3200.767	93.663	6.25		5-4	6-5	2080.667	144.085	0.54	
	2-1	2-2	3203.392	93.586	0.60		4-4	5-5	2089.641	143.466	9.97	
	2-1	1-1	3203.423	93.585	0.59		4-4	4-4	2089.642	143.466	7.67	
							4-4	3-3	2089.643	143.466	6.20	

TABLE 2—Continued

$N_{K_a K_c}$	$J$	$F^a$	Frequency (GHz)	Vacuum Wavelength ( $\mu\text{m}$ )	Line Strength
	5-5	4-4	2092.092	143.298	8.68
	5-5	5-5	2092.094	143.298	10.33
	5-5	6-6	2092.096	143.298	12.70
	3-3	3-4	2092.695	143.257	0.55
	3-3	2-3	2092.710	143.256	0.55
	3-3	4-4	2092.740	143.254	8.27
	3-3	3-3	2092.744	143.253	5.76
	3-3	3-2	2092.780	143.251	0.55
	3-3	4-3	2092.788	143.250	0.55
	4-5	5-6	2101.070	142.686	0.54
	4-3	5-4	2102.436	142.593	0.57
515-404 <sup>b</sup> .....	5-4	6-5	3988.597	75.162	6.60
	5-4	5-4	3988.599	75.162	5.36
	5-4	4-3	3988.600	75.162	4.35
	6-5	5-4	3988.664	75.161	5.62
	6-5	6-5	3988.665	75.161	6.68
	6-5	7-6	3988.667	75.161	7.93
	4-3	5-4	3989.390	75.147	5.52
	4-3	4-3	3989.395	75.147	4.23
	4-3	3-2	3989.396	75.147	3.23

<sup>a</sup> Where  $F$  is not given, the transition involves para-CH<sub>2</sub> levels with  $J = 0$  and no hyperfine structure.

<sup>b</sup> Transition not directly observed in the LMR spectrum.

<sup>c</sup> Note that this transition has been directly measured to high accuracy at zero field by Lovas, Suenram, and Evenson 1983.

with  $K_a + K_c = \text{an even number}$ ) are further split into levels with  $F = J - 1, J,$  and  $J + 1$  by hyperfine structure interactions involving the two <sup>1</sup>H nuclei. The energies were calculated using the parameters of Sears *et al.* (1982), and all levels below 200 cm<sup>-1</sup> (300 K) are included.

Table 2 lists all the transitions of significant intensity that occur among the levels of Table 1, and also some of the stronger high-frequency transitions from these levels to higher lying levels. Transitions are arranged in order of increasing energy of the lower state, beginning with 0<sub>00</sub>. The calculated transition strengths are defined by

$$S_{F'F''} = |\langle \gamma' F' \| D_q^{(1)}(\omega) \| \gamma'' F'' \rangle|^2, \quad (2)$$

where  $S_{F'F''}$  is the square of the reduced matrix element of the rotation matrix (Brink and Satchler 1968), and  $\gamma$  represents the additional quantum numbers needed to define a level ( $N, K_a, K_c,$  and  $J$ ). The absorption coefficient for a given transition is the product of  $S_{F'F''}$  and the transition frequency, the population difference of the two levels, the molecular column density, and the square of the dipole moment. Although the dipole moment of CH<sub>2</sub> has not been measured, the ab initio value of  $\mu = 0.57$  Debye (Bunker and Langhoff 1983) is thought to be rather accurate. Einstein  $A$  coefficients for spontaneous emission can also be calculated from  $S$  by means of

$$A_{i \rightarrow j} = (16\pi^3 \nu_{ij}^3 / 3\epsilon_0 hc^3) (2F_i + 1)^{-1} S_{ij} \mu^2. \quad (3)$$

The  $\nu_2$  (bending) fundamental band of CH<sub>2</sub> occurs in the 10  $\mu\text{m}$  region and has been studied by means of LMR spectroscopy with a CO<sub>2</sub> laser (Sears, Bunker, and McKellar 1981, 1982). The  $\nu_1$  and  $\nu_3$  stretching bands are much weaker than  $\nu_2$  (Bunker and Langhoff 1983) and have not yet been observed. They are expected to occur in the 3.3  $\mu\text{m}$  region

(Bunker and Jensen 1983). Since it is possible that CH<sub>2</sub> could be detected in astronomical sources using CO<sub>2</sub> laser heterodyne receivers (Betz 1982) or other sensitive infrared techniques, we present in Table 3 a list of  $\nu_2$  band transition frequencies and intensities. Here we have suppressed the hyperfine splittings, since they are certain to be masked by Doppler broadening at these wavelengths. As we have noted previously (Sears, Bunker, and McKellar 1982) the large geometry changes associated with the  $\nu_2$  vibration in CH<sub>2</sub> give rise to  $K_a$ -dependent intensity factors in the  $\nu_2$  band. The appropriate calculated dipole matrix elements (Bunker and Langhoff 1983) for the  $\nu_2$  band are: 0.096 debye for  $K_a = 0 \leftarrow 1$  transitions, and 0.042 debye for  $K_a = 1 \leftarrow 0$  transitions.

The transition frequencies given here that correspond to observed LMR transitions should be reliable to better than  $\pm 5$  MHz for Table 2 and  $\pm 0.0007$  cm<sup>-1</sup> for Table 3. Uncertainties for other transitions are somewhat difficult to assess because CH<sub>2</sub> is not especially well fitted by the conventional rotation-vibration Hamiltonian due to its large-amplitude anharmonic bending motion (see Sears, Bunker, and McKellar 1982 and Sears *et al.* 1982). We estimate that the transitions not observed by LMR have an uncertainty of about 10-20 MHz for Table 2 and about 0.003 cm<sup>-1</sup> for Table 3. In all cases, however, the relative spacings of the fine and hyperfine components of a given transition are considerably more reliable than this, and they provide distinctive spectral signatures for CH<sub>2</sub>.

TABLE 3  
CALCULATED TRANSITION FREQUENCIES FOR THE  $\nu_2$  BAND OF CH<sub>2</sub> (<sup>3</sup>B<sub>1</sub>)

$N_{K_a K_c}$	$J$	Wavenumber (cm <sup>-1</sup> )	Vacuum Wavelength ( $\mu\text{m}$ )	Line Strength
202-313 <sup>a</sup> .....	3-3	855.5017	11.689	1.30
	1-2	855.7121	11.686	7.14
	3-4	855.8048	11.685	15.38
	2-3	855.8582	11.684	10.67
	2-2	856.2306	11.679	1.36
101-212 <sup>a</sup> .....	0-1	869.7078	11.498	0.97
	2-2	869.8817	11.496	0.73
	2-3	870.0861	11.493	4.20
	1-2	870.2112	11.491	2.27
	1-1	870.4987	11.488	0.77
000-111.....	1-0	884.5517	11.305	1.98
	1-2	884.7570	11.303	9.99
	1-1	884.8878	11.301	6.03
404-413.....	3-4	891.3374	11.219	1.36
	5-4	891.3866	11.218	1.34
	3-3	891.6619	11.215	20.20
	5-5	891.6848	11.215	32.54
	4-4	891.7736	11.214	25.01
	4-5	892.0717	11.210	1.34
	4-3	892.0980	11.210	1.36
303-312.....	2-3	894.5923	11.178	0.57
	4-3	894.6807	11.177	0.56
	2-2	894.8911	11.175	4.50
	4-4	894.9328	11.174	8.57
	3-3	895.0546	11.173	5.97
	3-4	895.3068	11.169	0.56
	3-2	895.3535	11.169	0.57
202-211.....	1-2	897.0452	11.148	2.31
	3-2	897.2071	11.146	2.31
	1-1	897.2518	11.145	6.74
	3-3	897.3619	11.144	18.81
	2-2	897.5637	11.141	10.47

TABLE 3—Continued

$N_{k_1k_2}$	$J$	Wavenumber ( $\text{cm}^{-1}$ )	Vacuum Wavelength ( $\mu\text{m}$ )	Line Strength	$N_{k_1k_2}$	$J$	Wavenumber ( $\text{cm}^{-1}$ )	Vacuum Wavelength ( $\mu\text{m}$ )	Line Strength
101-110	2-3	897.7185	11.139	2.32	110-101*	2-2	1084.9024	9.217	0.70
	2-1	897.7702	11.139	2.32		2-3	1085.2517	9.214	4.10
	0-1	898.6681	11.128	1.03		1-1	1085.2705	9.214	0.75
	2-2	898.9522	11.124	3.77		0-1	1085.6208	9.211	0.99
	1-0	899.0030	11.123	1.00		1-1	1117.2373	8.951	0.73
202-111	2-1	899.1295	11.122	1.24	2-1	1117.4190	8.949	1.23	
	1-2	899.2817	11.120	1.23	1-2	1117.5597	8.948	1.24	
	1-1	899.4590	11.118	0.73	0-1	1117.6937	8.947	1.00	
	1-0	930.6542	10.745	1.00	2-2	1117.7415	8.947	3.77	
	1-1	930.9903	10.741	0.76	1-0	1118.0110	8.944	1.03	
303-212	3-2	931.0214	10.741	4.16	1-2	1118.5226	8.940	2.33	
	2-2	931.3780	10.737	0.71	3-2	1118.5815	8.940	2.32	
	2-1	931.5087	10.735	2.16	2-2	1118.7407	8.939	10.51	
	2-1	947.2338	10.557	1.17	3-3	1118.9307	8.937	18.89	
	4-3	947.2391	10.557	2.50	1-1	1119.0301	8.936	6.77	
212-303*	3-2	947.4087	10.555	1.72	2-3	1119.0900	8.936	2.32	
	2-3	1068.1776	9.362	1.68	2-1	1119.2483	8.935	2.32	
	3-4	1068.3398	9.360	2.45	1-1	1131.9042	8.835	6.03	
111-202	1-2	1068.3415	9.360	1.14	2-1	1132.0437	8.834	9.99	
	1-2	1084.7630	9.219	2.13	0-1	1132.2545	8.832	1.98	

\* Transition not directly observed in the LMR spectrum.

## REFERENCES

- Betz, A. L. 1982, in *Laser Spectroscopy V*, ed. A. R. W. McKellar, T. Oka, and B. P. Stoicheff (New York: Springer-Verlag), p. 81.
- Brink, D. M., and Satchler, G. R. 1968, *Angular Momentum* (Oxford: Oxford University Press).
- Bunker, P. R., and Jensen, P. 1983, *J. Chem. Phys.*, **79**, 1224.
- Bunker, P. R., and Langhoff, S. R. 1983, *J. Molec. Spectrosc.*, to be published.
- Inglesias, E. 1977, *Ap. J.*, **218**, 697.
- Lovas, F. J., Suenram, R. D., and Evenson, K. 1983, *Ap. J. (Letters)*, **267**, L131.
- Prasad, S. S., and Huntress, W. J. 1980, *Ap. J.*, **239**, 151.
- Sears, T. J., Bunker, P. R., and McKellar, A. R. W. 1981, *J. Chem. Phys.*, **75**, 4731.
- , 1982, *J. Chem. Phys.*, **77**, 5363.
- Sears, T. J., Bunker, P. R., McKellar, A. R. W., Evenson, K. M., Jennings, D. A., and Brown, J. M. 1982, *J. Chem. Phys.*, **77**, 5348.

J. M. BROWN: Department of Chemistry, Southampton University, Southampton, SO9 5NH, England, U.K.

P. R. BUNKER, A. R. W. MCKELLAR, and TREVOR J. SEARS: Herzberg Institute of Astrophysics, National Research Council of Canada, Ottawa, ON K1A 0R6, Canada

K. M. EVENSON: National Bureau of Standards, Boulder, CO 80303